Structural Engineering and Mechanics, *Vol. 66, No. 6 (2018) 761-769*
DOI: https://doi.org/10.12989/sem.2018.66.6.761

Mechanical buckling analysis of hybrid laminated composite plates under different boundary conditions

Adim Belkacem*[1,2], Hassaine Daouadji Tahar[2,3], Rabahi Abderrezak[2,3], Benhenni Mohamed Amine[2,3], Zidour Mohamed[2,3] and Abbes Boussad[4]

[1]*Département des Sciences et Technologies, Centre Universitaire El Wancharissi - Tissemsilt, Algérie*
[2]*Laboratoire de Géomatique et Développement Durable, Université Ibn Khaldoun de Tiaret Algérie*
[3]*Département de Génie Civil, Université Ibn Khaldoun Tiaret; BP 78 Zaaroura, 14000 Tiaret, Algérie*
[4]*Laboratoire GRESPI - Campus du Moulin de la Housse BP 1039 - 51687 Reims Cedex 2, France*

(Received January 22, 2017, Revised April 3, 2018, Accepted April 5, 2018)

Abstract. In this paper, we study the Carbon/Glass hybrid laminated composite plates, where the buckling behavior is examined using an accurate and simple refined higher order shear deformation theory. This theory takes account the shear effect, where shear deformation and shear stresses will be considered in determination of critical buckling load under different boundary conditions. The most interesting feature of this new kind of hybrid laminated composite plates is that the possibility of varying components percentages, which allows us for a variety of plates with different materials combinations in order to overcome the most difficult obstacles faced in traditional laminated composite plates like (cost and strength). Numerical results of the present study are compared with three-dimensional elasticity solutions and results of the first-order and the other higher-order theories issue from the literature. It can be concluded that the proposed theory is accurate and simple in solving the buckling behavior of hybrid laminated composite plates and allows to industrials the possibility to adjust the component of this new kind of plates in the most efficient way (reducing time and cost) according to their specific needs.

Keywords: hybrid plates; laminated composite plates; higher-order shear deformation theory; transverse shear; buckling

1. Introduction

For the time being, laminated composite plates attract more and more attention every day, thanks to their various features, strength and good mechanical resistance. However, it costs a lot of money in order to determine their mechanical and physical characteristics throw various experiments, this impediment pushed scientists to adopt mathematical solutions to create models that represents the real behavior of composite plates, beam and shells (Mahi 2015, Attia 2018, Bounouara 2016, Zine 2018, Chikh 2017). The most interesting of these mathematical models are those which takes into account the shear effect in term of deducing the deformations and stresses such as: The first order shear deformation theory introduced by Reissner (1945) and Mindlin (1951) takes into account the shear effect in deformations and stresses; however, this presented a huge deficiency due its linear distribution of the shear stresses throw the thickness which requires the introduction of the shear correction factors Srivinas (1970), Whitney (1973), Bert (1974). In order to remedy this previous handicap, a numerous high order shear deformation theories has seen the light of day, starting with Librescu (1967), Levinson (1980), Bhimaraddi and Stevens (1984), Reddy (1984), Ren (1986), Kant and Pandya (1988). The refined high order shear deformation theory has appeared to simplify the mathematical formulation by reducing the number of unknown functions Adim (2016a), Abdelhak (2015), Abdelhak (2016), Daouadji (2015), Nedri (2014), Thai (2013), Tlidji (2014), Beldjelili (2016), Tounsi (2013), Bouderba (2013), Zidi (2014), Ait Yahia (2015), Boukhari (2016), Bellifa (2016), Youcef (2018), Zemri (2015), Ahouel (2016), Larbi Chaht (2015), Belkorissat (2015), Khetir (2017), Besseghier (2017), Al-Basyouni (2015). The most interesting feature of this refined theory is that it does not require shear correction factor, and has strong similarities with the classical plate theory in some aspects such as simplicity and ease of resolving.

The stretching effect was introduced in the displacement field for the purpose of taking into account the deformation in the thickness, Bourada (2015), Hebali (2014), Bennoun (2016), Bousahla (2014), Draiche (2016), Hamidi (2015), Belabed (2014), Abualnour (2018), Benchohra (2018). In the literature we can find a numerous research talking about the buckling and post-buckling behavior and how to analyze this phenomena that touches directly the plate's stability, Bousahla (2016), Bellifa (2017a), El-Haina (2017), Menasria (2017), Bouderba (2016), Ait Amar (2014), Abdelaziz (2017), Bellifa (2017b), Yazid (2018).

In this paper, a simple refined theory is used to study the buckling behavior of Carbon/Glass hybrid laminated composite plates under mechanical load. This theory allows for a parabolic distributions of transverse shear stresses across the plate thickness and satisfies zero shear stress conditions at the top and bottom surfaces of the hybrid plate and does not require any shear correction factors. The

*Corresponding author, Ph.D.
E-mail: adim.belkacem@gmail.com

ISSN: 1225-4568 (Print), 1598-6217 (Online)

equilibrium equations are derived from virtual displacement's principle. The critical buckling loads are found using the Navier's solution. For validation purposes, the results obtained using the present theory are compared with results of other higher-order theories from the literature.

2. Material properties

In addition of the matrix, most composite structures are made of one type of fibers which means that the composite properties depend on this particular type of fibers. If this fiber presents a handicap like fragility or low strength, the all structure will be vulnerable to damage or failure.

Hybrid composite plates are made of more than one type of fibers, generally two types; this promising technology provides a various features like reducing manufacturing cost or improving a specific quality of one of the fibers such as (wear resistance, vibration damping, toughness, strength, temperature resistance, Electrical conductivity, etc.).

In this study a laminated hybrid Carbon/Glass epoxy plate is considered, the longitudinal and transversal Young moduli are given Vaseliev (2001) by

$$E_1 = E_f^1\ V_f^1 + E_f^2\ V_f^2 + E_m\ V_m \tag{1}$$

Where E_1 is longitudinal Young's modulus. E_f^1, E_f^2 and E_m are the Young's moduli of the first type of fibers, the second type of fibers and the matrix respectively. V_f^1, V_f^2 and V_m are the volume fraction of the first type of fibers, the second type of fibers and the matrix, respectively, where

$$V_f^1 + V_f^2 + V_m = 1 \ \text{ and } \ V_f^1 + V_f^2 = V_f \tag{2}$$

Assuming that

$$w_f = \frac{V_f^1}{V_f} \tag{3}$$

Where w_f is the first fiber percentage over the total fiber's volume fraction.

By replacing Eq. (3) into Eq. (1) we obtain

$$E_1 = V_f\,[E_f^1\ w_f + E_f^2\ (1-w_f)] + E_m\ V_m \tag{4}$$

Using the same approach, the Poisson's coefficient can be calculated by

$$\nu_{12} = V_f\,[\nu_f^1\ w_f + \nu_f^2\ (1-w_f)] + \nu_m\ V_m \tag{5}$$

The shear modulus of the fibers and the matrix are expressed in Berthelot (2012) by

$$G_m = \frac{E_m}{2\,(1+\nu_m)} \tag{6a}$$

$$G_f^1 = \frac{E_f^1}{2\,(1+\nu_f^1)} \tag{6b}$$

$$G_f^2 = \frac{E_f^2}{2\,(1+\nu_f^2)} \tag{6c}$$

Where G_f^1, G_f^2 and G_m are the shear modulus of the first type of fibers, the second type of fibers and the matrix, respectively, also the total shear modulus of fibers is given by

$$G_f = G_f^1\ w_f + G_f^2\ (1-w_f) \tag{7}$$

The compressibility modulus of the fibers and the matrix are given as

$$k_f = \frac{E_f^1\ w_f}{3\,(1-2\nu_f^1)} + \frac{E_f^2\,(1-w_f)}{3\,(1-2\nu_f^2)} \tag{8a}$$

$$k_m = \frac{E_m}{3\,(1-2\nu_m)} \tag{8b}$$

The lateral compressibility modulus of the fibers and the matrix are given as

$$K_f = k_f + \frac{G_f}{3} \tag{9a}$$

$$K_m = k_m + \frac{G_m}{3} \tag{9b}$$

The shear moduli of the plate are

$$G_{23} = G_m \left(1 + \frac{V_f}{\dfrac{G_m}{G_f - G_m} + V_m \dfrac{k_m + 7G_m/3}{2k_m + 8G_m/3}} \right) \tag{10a}$$

$$G_{12} = G_m \frac{G_f(1+V_f) + G_m(1-V_f)}{G_f(1-V_f) + G_m(1+V_f)} \tag{10b}$$

$$G_{13} = G_{12} \tag{10c}$$

The lateral compressibility modulus of the plate is given as

$$K_L = K_m + \frac{V_f}{\dfrac{1}{k_f - k_m + (G_f - G_m)/3} + \dfrac{1-V_f}{k_m + (4/3)G_m}} \tag{11}$$

Using equations from (4) to (11), the transversal Young's modulus is given as follows

$$E_2 = \frac{2}{\dfrac{1}{2K_L} + \dfrac{1}{2G_{23}} + \dfrac{2(\nu_{12})^2}{E_1}} \tag{12}$$

3. Kinematics

Based on the assumptions made By Daouadji (2017), the displacement field can be obtained as

$$u(x,y,z) = u_0(x,y) - z\frac{\partial w_b}{\partial x} - \left[z - \sin\left(\frac{\pi z}{h}\right)\right]\frac{\partial w_s}{\partial x}$$
$$v(x,y,z) = v_0(x,y) - z\frac{\partial w_b}{\partial y} - \left[z - \sin\left(\frac{\pi z}{h}\right)\right]\frac{\partial w_s}{\partial y} \qquad (13)$$
$$w(x,y,z) = w_b(x,y) + w_s(x,y)$$

Where **u** and **v** are the mid-plane displacements of the plate in the "x" and "y" direction, respectively; w_b and w_s are the bending and shear components of transverse displacement, respectively.

The strains associated with the displacements in Eq. (13) are

$$\begin{aligned} \varepsilon_x &= \varepsilon_x^0 + z\,k_x^b + f\,k_x^s \\ \varepsilon_y &= \varepsilon_y^0 + z\,k_y^b + f\,k_y^s \\ \gamma_{xy} &= \gamma_{xy}^0 + z\,k_{xy}^b + f\,k_{xy}^s \\ \gamma_{yz} &= g\,\gamma_{yz}^s \\ \gamma_{xz} &= g\,\gamma_{xz}^s \\ \varepsilon_z &= 0 \end{aligned} \qquad (14)$$

Where

$$\varepsilon_x^0 = \frac{\partial u_0}{\partial x}, \quad k_x^b = -\frac{\partial^2 w_b}{\partial x^2}, \quad k_x^s = -\frac{\partial^2 w_s}{\partial x^2},$$
$$\varepsilon_y^0 = \frac{\partial v_0}{\partial y}, \ \gamma_{xy}^0 = \frac{\partial u_0}{\partial y} + \frac{\partial v_0}{\partial x}, \ k_{xy}^b = -2\frac{\partial^2 w_b}{\partial x \partial y},$$
$$k_{xy}^s = -2\frac{\partial^2 w_s}{\partial x \partial y}, \quad k_y^b = -\frac{\partial^2 w_b}{\partial y^2}, \quad k_y^s = -\frac{\partial^2 w_s}{\partial y^2}, \qquad (15)$$
$$\gamma_{yz}^s = \frac{\partial w_s}{\partial y}, \quad \gamma_{xz}^s = \frac{\partial w_s}{\partial x}, \ g(z) = 1 - f'(z) \ \text{and}$$
$$f'(z) = \frac{df(z)}{dz}$$

4. Constitutive equations

Since the Hybrid laminated plates is made of several orthotropic layers with their material axes oriented arbitrarily with respect to the laminate coordinates, the constitutive equations of each layer must be transformed to the laminate coordinates (x,y,z). The stress-strain relations in the laminate coordinates of the ***kth*** layer are given as

$$\begin{Bmatrix} \sigma_x \\ \sigma_y \\ \sigma_{xy} \\ \sigma_{yz} \\ \sigma_{xz} \end{Bmatrix}^{(k)} = \begin{bmatrix} \bar{Q}_{11} & \bar{Q}_{12} & \bar{Q}_{16} & 0 & 0 \\ \bar{Q}_{12} & \bar{Q}_{22} & \bar{Q}_{26} & 0 & 0 \\ \bar{Q}_{16} & \bar{Q}_{26} & \bar{Q}_{66} & 0 & 0 \\ 0 & 0 & 0 & \bar{Q}_{44} & \bar{Q}_{45} \\ 0 & 0 & 0 & \bar{Q}_{45} & \bar{Q}_{55} \end{bmatrix}^{(k)} \begin{Bmatrix} \varepsilon_x \\ \varepsilon_y \\ \gamma_{xy} \\ \gamma_{yz} \\ \gamma_{xz} \end{Bmatrix}^{(k)} \qquad (16)$$

Where $\bar{Q}_{ij}$ are the transformed material constants detailed in Adim (2016c).

5. Governing equations

The strain energy of the hybrid composite plate can be written as

$$U = \frac{1}{2}\int_V \sigma_{ij}\varepsilon_{ij}dV = \frac{1}{2}\int_V (\sigma_x\varepsilon_x + \sigma_y\varepsilon_y + \sigma_{xy}\gamma_{xy} + \sigma_{yz}\gamma_{yz} + \sigma_{xz}\gamma_{xz})dV \qquad (17)$$

The work done by applied forces can be written as

$$V = \frac{1}{2}\int_A \left[N_x^0 \frac{\partial^2 (w_b + w_s)}{\partial x^2} + N_y^0 \frac{\partial^2 (w_b + w_s)}{\partial y^2} + 2N_{xy}^0 \frac{\partial^2 (w_b + w_s)}{\partial x \partial y}\right] dxdy \qquad (18)$$

Where N_x^0, N_y^0 and N_{xy}^0 are in-plane distributed forces.

Virtual work principle is used here in order to derive the equilibrium equations appropriate to the displacement field and the constitutive equations. The principle can be stated in analytical form as

$$U + V = 0 \qquad (19)$$

Substituting Eqs. (16) and (18) into Eq. (19) and integrating the equation by parts, collecting the coefficients of δu_0, δv_0, δw_b and δw_s, the equilibrium equations for the hybrid laminated plate are obtained as follows

$$\begin{aligned} &\delta u_0 : \frac{\partial N_x}{\partial x} + \frac{\partial N_{xy}}{\partial y} = 0 \\ &\delta v_0 : \frac{\partial N_{xy}}{\partial x} + \frac{\partial N_y}{\partial y} = 0 \\ &\delta w_b : \frac{\partial^2 M_x^b}{\partial x^2} + 2\frac{\partial^2 M_{xy}^b}{\partial x \partial y} + \frac{\partial^2 M_y^b}{\partial y^2} + N(w) = 0 \\ &\delta w_s : \frac{\partial^2 M_x^s}{\partial x^2} + 2\frac{\partial^2 M_{xy}^s}{\partial x \partial y} + \frac{\partial^2 M_y^s}{\partial y^2} + \frac{\partial Q_{xz}^s}{\partial x} + \frac{\partial Q_{yz}^s}{\partial y} + N(w) = 0 \end{aligned} \qquad (20)$$

Where $N(w)$ is defined by

$$N(w) = N_x^0 \frac{\partial^2 (w_b + w_s)}{\partial x^2} + N_y^0 \frac{\partial^2 (w_b + w_s)}{\partial y^2} + 2N_{xy}^0 \frac{\partial^2 (w_b + w_s)}{\partial x \partial y} \qquad (21)$$

6. Exact solution for antisymmetric cross-ply laminates

For antisymmetric cross-ply laminates, the following plate stiffnesses are identically zero

$$\begin{gathered} A_{16} = A_{26} = D_{16} = D_{26} = D_{16}^s = D_{26}^s = H_{16}^s = H_{26}^s = 0, \\ B_{22} = -B_{11}, \ B_{22}^s = -B_{11}^s \\ B_{12} = B_{26} = B_{16} = B_{66} = B_{12}^s = B_{16}^s = B_{26}^s = B_{66}^s = A_{45}^s = 0 \end{gathered} \qquad (22)$$

The exact solution of Eq. (20) for the antisymmetric cross-ply laminated plate under various boundary conditions can be constructed according to Adim (2016b). The boundary conditions for an arbitrary edge with simply supported and clamped edge conditions are:

- Clamped (C)

Table 1 The admissible functions $X_m(x)$ and $Y_n(y)$

	Boundary conditions		The functions $X_m(x)$ and $Y_n(y)$	
	At x=0, a	At y=0, b	$X_m(x)$	$Y_n(y)$
SSSS	$X_m(0)=X_m''(0)=0$ $X_m(a)=X_m''(a)=0$	$Y_n(0)=Y_n''(0)=0$ $Y_n(b)=Y_n''(b)=0$	$\sin(\alpha x)$	$\sin(\beta y)$
CSSS	$X_m(0)=X_m'(0)=0$ $X_m(a)=X_m''(a)=0$	$Y_n(0)=Y_n''(0)=0$ $Y_n(b)=Y_n''(b)=0$	$\sin(\alpha x)[\cos(\alpha x)-1]$	$\sin(\beta y)$
CSCS	$X_m(0)=X_m'(0)=0$ $X_m(a)=X_m''(a)=0$	$Y_n(0)=Y_n'(0)=0$ $Y_n(b)=Y_n''(b)=0$	$\sin(\alpha x)[\cos(\alpha x)-1]$	$\sin(\beta y)[\cos(\beta y)-1]$
CCSS	$X_m(0)=X_m'(0)=0$ $X_m(a)=X_m'(a)=0$	$Y_n(0)=Y_n''(0)=0$ $Y_n(b)=Y_n''(b)=0$	$\sin^2(\alpha x)$	$\sin(\beta y)$
CCCC	$X_m(0)=X_m'(0)=0$ $X_m(a)=X_m'(a)=0$	$Y_n(0)=Y_n'(0)=0$ $Y_n(b)=Y_n'(b)=0$	$\sin^2(\alpha x)$	$\sin^2(\beta y)$
FFCC	$X_m''(0)=X_m'''(0)=0$ $X_m''(a)=X_m'''(a)=0$	$Y_n(0)=Y_n'(0)=0$ $Y_n(b)=Y_n'(b)=0$	$\cos^2(\alpha x)[\sin^2(\alpha x)+1]$	$\sin^2(\beta y)$

$(\,)'$ denotes the derivative with respect to the corresponding coordinates.

$$u_0 = v_0 = w_b = w_s = \frac{\partial w_b}{\partial x} = \frac{\partial w_b}{\partial y} = \frac{\partial w_s}{\partial x} = \frac{\partial w_s}{\partial y} = 0 \quad \text{at} \quad x = 0, a \quad \text{and} \quad y = 0, b \tag{23}$$

• Simply supported (S)

$$v_0 = w_b = w_s = \frac{\partial w_b}{\partial y} = \frac{\partial w_s}{\partial y} = 0 \quad \text{at} \quad x = 0, a \tag{24a}$$

$$u_0 = w_b = w_s = \frac{\partial w_b}{\partial x} = \frac{\partial w_s}{\partial x} = 0 \quad \text{at} \quad y = 0, b \tag{24b}$$

The boundary conditions in Eq. (23) and (24) are satisfied by the following expansions

$$\begin{aligned} u_0 &= U_{mn} X_m'(x)\, Y_n(y) \\ v_0 &= V_{mn}\, X_m(x)\, Y_n'(y) \\ w_b &= W_{bmn} X_m(x)\, Y_n(y) \\ w_s &= W_{smn} X_m(x)\, Y_n(y) \end{aligned} \tag{25}$$

Where U_{mn}, V_{mn}, W_{bmn} and W_{smn} unknown parameters must be determined. The functions $X_m(x)$ and $Y_n(y)$ are suggested here to satisfy at least the geometric boundary conditions given in Eqs. (23) and (24) and represent approximate shapes of the deflected surface of the plate. These functions, for the different cases of boundary conditions, are listed in Table 1, with $\alpha = \frac{m\pi}{a}$ and $\beta = \frac{n\pi}{b}$.

Substituting Eqs. (25) and (22) into Eq. (20), the exact solution of antisymmetric cross-ply laminates can be determined from equations

$$\begin{bmatrix} s_{11} & s_{12} & s_{13} & s_{14} \\ s_{21} & s_{22} & s_{23} & s_{24} \\ s_{31} & s_{32} & s_{33}+k & s_{34}+k \\ s_{41} & s_{42} & s_{43}+k & s_{44}+k \end{bmatrix} \begin{Bmatrix} U_{mn} \\ V_{mn} \\ W_{bmn} \\ W_{smn} \end{Bmatrix} = \begin{Bmatrix} 0 \\ 0 \\ 0 \\ 0 \end{Bmatrix} \tag{26}$$

Where

$$s_{11} = \int_0^a\int_0^b \left(A_{11} X_m''' Y_n + A_{66} X_m' Y_n''\right) X_m' Y_n \, dxdy$$

$$s_{12} = \int_0^a\int_0^b \left(A_{12} + A_{66}\right) X_m' Y_n'' X_m' Y_n \, dxdy$$

$$s_{13} = -\int_0^a\int_0^b \left[B_{11} X_m'' Y_n + \left(B_{12} + 2B_{66}\right) X_m' Y_n''\right] X_m' Y_n \, dxdy$$

$$s_{14} = -\int_0^a\int_0^b \left[B_{11}^s X_m'' Y_n + \left(B_{12}^s + 2B_{66}^s\right) X_m' Y_n''\right] X_m' Y_n \, dxdy \tag{27a}$$

$$s_{21} = \int_0^a\int_0^b \left(A_{12} + A_{66}\right) X_m'' Y_n' X_m Y_n' \, dxdy$$

$$s_{22} = \int_0^a\int_0^b \left(A_{22} X_m Y_n''' + A_{66} X_m'' Y_n'\right) X_m Y_n' \, dxdy$$

$$s_{23} = -\int_0^a\int_0^b \left[B_{22} X_m Y_n''' + \left(B_{12} + 2B_{66}\right) X_m'' Y_n'\right] X_m Y_n' \, dxdy$$

$$s_{24} = -\int_0^a\int_0^b \left[B_{22}^s X_m Y_n''' + \left(B_{12}^s + 2B_{66}^s\right) X_m'' Y_n'\right] X_m Y_n' \, dxdy$$

$$s_{31} = \int_0^a\int_0^b \left[B_{11} X_m'''' Y_n + \left(B_{12} + 2B_{66}\right) X_m'' Y_n''\right] X_m Y_n \, dxdy$$

$$s_{32} = \int_0^a\int_0^b \left[B_{22} X_m Y_n'''' + \left(B_{12} + 2B_{66}\right) X_m'' Y_n''\right] X_m Y_n \, dxdy$$

$$s_{33} = \int_0^a\int_0^b -\left[D_{11} X_m'''' Y_n + 2\left(D_{12} + 2D_{66}\right) X_m'' Y_n'' + D_{22} X_m Y_n''''\right] X_m Y_n \, dxdy$$

$$s_{34} = \int_0^a\int_0^b -\left[D_{11}^s X_m'''' Y_n + 2\left(D_{12}^s + 2D_{66}^s\right) X_m'' Y_n'' + D_{22}^s X_m Y_n''''\right] X_m Y_n \, dxdy \tag{27b}$$

$$s_{41} = \int_0^a\int_0^b \left[B_{11}^s X_m'''' Y_n + \left(B_{12}^s + 2B_{66}^s\right) X_m'' Y_n''\right] X_m Y_n \, dxdy$$

$$s_{42} = \int_0^a\int_0^b \left[B_{22}^s X_m Y_n'''' + \left(B_{12}^s + 2B_{66}^s\right) X_m'' Y_n''\right] X_m Y_n \, dxdy$$

$$s_{43} = \int_0^a\int_0^b -\left[D_{11}^s X_m'''' Y_n + 2\left(D_{12}^s + 2D_{66}^s\right) X_m'' Y_n'' + D_{22}^s X_m Y_n''''\right] X_m Y_n \, dxdy$$

$$s_{44} = \int_0^a\int_0^b -\left[H_{11}^s X_m'''' Y_n + 2\left(H_{12}^s + 2H_{66}^s\right) X_m'' Y_n'' + H_{22}^s X_m Y_n'''' - A_{55}^s X_m'' Y_n - A_{44}^s X_m Y_n''\right] X_m Y_n \, dxdy$$

$$k = N_{cr} \int_0^a\int_0^b \left(\gamma_1 X_m'' Y_n + \gamma_2 X_m Y_n''\right) X_m Y_n \, dxdy$$

$$N_x^0 = \gamma_1 N_{cr}, \quad N_y^0 = \gamma_2 N_{cr}, \text{ and } \quad N_{xy}^0 = 0 \tag{28}$$

And

Table 2 Dimensionless uniaxial critical buckling load $\bar{N}$ of simply supported antisymmetric cross-ply $(0/90)_n$ square composite laminates

Theory	Number of layers		
	$(0/90)_2$	$(0/90)_3$	$(0/90)_5$
Exact Noor (1975)	21.2796	23.6689	24.9636
Reddy (1984)	22.5790	24.4596	25.4225
Adim (2016c)	22.5821	24.4605	25.4223
Present	22.5530	24.4607	25.4354
FSDT Whitney(1970)	22.8060	24.5777	25.4500

Table 3 The volume fraction $\mathbf{V_f}$ effect on the variation of critical buckling load $\bar{N}$ of a square antisymmetric cross-ply $(0/90)$ hybrid composite laminates

Fiber's percentages (%)		V_f								
Carbon	Glass	0.3	0.35	0.4	0.45	0.5	0.55	0.6	0.65	0.7
0	100	4.5340	4.5948	4.6346	4.6549	4.6566	4.6405	4.6068	4.5555	4.4859
10	90	4.8254	4.9013	4.9503	4.9743	4.9745	4.9520	4.9072	4.8405	4.7514
20	80	5.1036	5.1947	5.2531	5.2809	5.2798	5.2512	5.1958	5.1143	5.0065
30	70	5.3731	5.4792	5.5468	5.5783	5.5759	5.5410	5.4757	5.3787	5.2522
40	60	5.6365	5.7547	5.8340	5.8691	5.8652	5.8241	5.7474	5.6361	5.4907
50	50	5.8952	6.0308	6.1162	6.1549	6.1493	6.1019	6.0144	5.8881	5.7238
60	40	6.1503	6.3003	6.3944	6.4364	6.4293	6.3756	6.2773	6.1360	5.9526
70	30	6.4022	6.5665	6.6692	6.7145	6.7058	6.6457	6.5366	6.3803	6.1780
80	20	6.6514	6.8298	6.9410	6.9896	6.9791	6.9127	6.7930	6.6218	6.4006
90	10	6.8982	7.0905	7.2101	7.2618	7.2497	7.1771	7.0467	6.8607	6.6207
100	0	7.1427	7.3488	7.4766	7.5315	7.5177	7.4389	7.2980	7.0973	6.8386

Table 4 The effect of side to thickness ratio a/h on critical buckling load $\bar{N}$ of a square antisymmetric cross-ply $(0/90)_4$ hybrid composite laminates

Fiber's percentages (%)		a/h				
Carbon	Glass	5	10	20	50	100
0	100	3.8508	4.6549	4.9125	4.9899	5.0012
10	90	4.0741	4.9743	5.2668	5.3551	5.3679
20	80	4.2865	5.2809	5.6081	5.7072	5.7217
30	70	4.4899	5.5783	5.9408	6.0510	6.0671
40	60	4.6859	5.8691	6.2677	6.3893	6.4072
50	50	4.8759	6.1549	6.5905	6.7240	6.7436
60	40	5.0604	6.4364	6.9103	7.0561	7.0774
70	30	5.2310	6.7145	7.2277	7.3862	7.4094
80	20	5.4152	6.9896	7.5432	7.7148	7.7310
90	10	5.5862	7.2618	7.8572	8.0423	8.0695
100	0	5.7534	7.5315	8.1697	8.3689	8.3981

Table 5 The stacking effect on the critical buckling load $\bar{N}$ of a square antisymmetric cross-ply $(0/90)_n$ hybrid composite laminates

Number of layers	a/h	Fiber's percentages (%)			
		100% Glass	25% Carbon + 75% Glass	50% Carbon + 50% Glass	100% Carbon
$(0/90)_1$	5	3.8508	4.3892	4.8759	5.7534
	10	4.6549	5.4306	6.1549	7.5315
	20	4.9125	5.7753	6.5905	8.1697
	100	5.0012	5.8952	6.7436	8.3981
$(0/90)_2$	5	4.5863	5.7549	6.7016	8.1378
	10	5.8510	7.9322	9.8659	13.3391
	20	6.2864	8.7664	11.1982	15.9098
	100	6.4399	9.0722	11.7051	16.9588
$(0/90)_3$	5	4.7311	6.0156	7.0429	8.5763
	10	6.0748	8.3923	10.5378	14.3616
	20	6.5414	9.3187	12.0446	17.3176
	100	6.7064	9.6605	12.6235	18.5429
$(0/90)_4$	5	4.7827	6.1087	7.1650	8.734491
	10	6.1534	8.5538	10.7735	14.7198
	20	6.6307	9.5121	12.3409	17.8100
	100	6.7996	9.8664	12.9450	19.0973
$(0/90)_5$	5	4.8068	6.1521	7.2220	8.8087
	10	6.1898	8.6287	10.8827	14.8859
	20	6.6720	9.6016	12.4781	18.0379
	100	6.8428	9.9617	13.0938	19.3539
$(0/90)_6$	5	4.8199	6.1758	7.2532	8.8492
	10	6.2096	8.6694	10.9421	14.9761
	20	6.6945	9.6503	12.5526	18.1617
	100	6.8663	10.0135	13.1746	19.4933
$(0/90)_8$	5	4.8330	6.1994	7.2842	8.8897
	10	6.2294	8.7099	11.0012	15.0659
	20	6.7168	9.6986	12.6268	18.2848
	100	6.8896	10.0649	13.2550	19.6318
$(0/90)_{16}$	5	4.8465	6.2222	7.3143	8.9290
	10	6.2484	8.7490	11.0582	15.1526
	20	6.7384	9.7453	12.6982	18.4036
	100	6.9120	10.1146	13.3325	19.7655

7. Numerical results and discussion

In this study, a buckling analysis of a Carbon/Glass hybrid laminated composite plate is presented using a refined shear deformation theory. The exact solution is used here to determine the critical buckling loads. For validation purposes, the mechanical characteristics of the composite plate used are: Material 1 Noor (1975): $\mathbf{E_1 = 40E_2, G_{12} = G_{13} = 0{,}6E_2, G_{23} = 0{,}5E_2, \nu_{12} = 0{,}25}$. Where, the results obtained by the present theory are compared with those of the FSDT Whitney (1970), Adim (2016c), Reddy (1984) and exact solution of three-dimensional elasticity Noor (1975). For convenience, the dimensionless critical buckling load is obtained using the following formula

$$\bar{N} = N_{cr}\left(\frac{a^2}{E_2 h^3}\right) \tag{29}$$

Table 6 The effect of boundary conditions on critical buckling load $\bar{N}$ of a square antisymmetric cross-ply $(0/90)_4$ hybrid (Carbon/Glass) composite laminates

w_f (%)		Boundary Conditions					
Carbon	Glass	SSSS	CSSS	CSCS	SSCC	CCCC	FFCC
0	100	6.1534	8.1311	12.4298	11.0248	16.6528	20.6684
10	90	7.1338	9.4445	14.3314	12.8132	19.1701	23.6520
20	80	8.0879	10.6891	16.1094	14.4746	21.4486	26.2999
30	70	9.0123	11.8652	17.7680	16.0159	23.5123	28.6567
40	60	9.9072	12.9769	19.3171	17.4482	25.3890	30.7668
50	50	10.7735	14.0291	20.7668	18.7825	27.1026	32.6672
60	40	11.6126	15.0263	22.1263	20.0285	28.6740	34.3884
70	30	12.4256	15.9727	23.4037	21.1947	30.1205	35.9555
80	20	13.2138	16.8722	24.6066	22.2888	31.4569	37.389
90	10	13.9781	17.7282	25.7412	23.3173	32.6958	38.7061
100	0	14.7198	18.5439	26.8136	24.2863	33.8478	39.921

Table 7 The effect of aspect ratio a/b on critical buckling load $\bar{N}$ of a square antisymmetric cross-ply $(0/90)_4$ hybrid (Carbon/Glass) composite laminates

Boundary conditions	a/b	a/h				
		5	10	20	50	100
SSSS	0.5	3.8921	5.4974	6.1342	6.3402	6.3708
	1	7.1650	10.7735	12.3409	12.8662	12.9450
	2	29.1427	62.2740	87.9580	99.5331	101.4435
CSSS	0.5	5.6938	10.4632	13.2945	14.3895	14.5610
	1	7.7946	14.0291	17.6056	18.9648	19.1765
	2	20.8632	45.6012	65.6310	74.9142	76.4621
CSCS	0.5	6.1151	11.1783	14.1578	15.3048	15.4843
	1	10.6172	20.7668	27.4670	30.2106	30.6486
	2	36.2542	97.8417	178.8522	234.0374	244.8775
CCSS	0.5	6.8096	14.3243	19.9796	22.4813	22.8915
	1	9.4525	18.7825	25.1144	27.7482	28.1708
	2	24.4796	55.0082	81.1177	93.6698	95.7918
CCCC	0.5	7.1750	15.1065	21.0857	23.7336	24.1679
	1	12.1511	27.1026	39.7003	45.6956	46.7053
	2	39.5483	114.7997	241.7045	354.2980	379.7374
FFCC	0.5	8.2587	19.6771	30.7139	36.5054	37.5187
	1	13.6890	32.6672	51.0765	60.7625	62.4589
	2	43.5974	127.2024	271.4062	402.8444	433.0107

Unless cited otherwise the following configurations are used: **a/h**=10, **a/b**=1, $\mathbf{V_f}$ =0.45

For the parametric study we use a hybrid plate made of two types of fibers, the first type of fiber is carbon and the second one is glass, and the matrix is made of epoxy, their material properties are cited in Berthelot (2012) as follows

Carbon fiber: $E_f = 380$ GPa , $\nu_f = 0.33$

Glass fiber: $E_f = 86$ GPa , $\nu_f = 0.22$

Matrix (Epoxy): $E_m = 3.45$GPa , $\nu_m = 0.3$

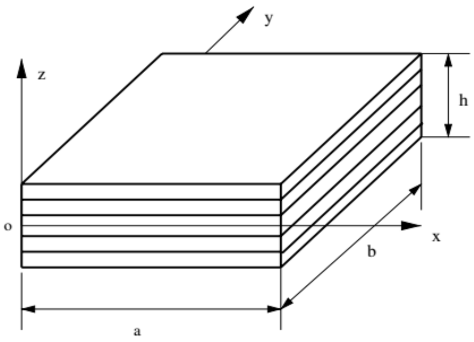

Fig. 1 Coordinate system used for a typical laminated composite plate, Jian (2004)

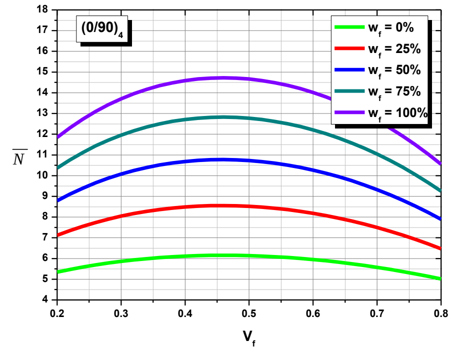

Fig. 2 The volume fraction V_f effect on the critical buckling load $\bar{N}$ of a square antisymmetric hybrid composite laminates

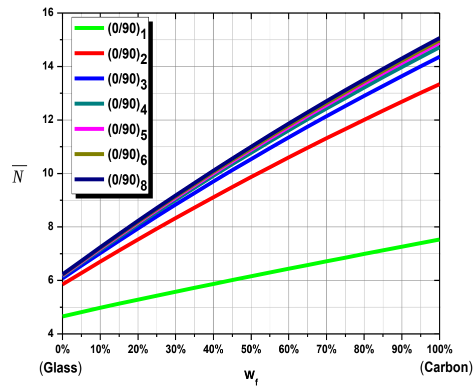

Fig. 3 The stacking effect on the critical buckling load $\bar{N}$ of a square antisymmetric hybrid composite laminates

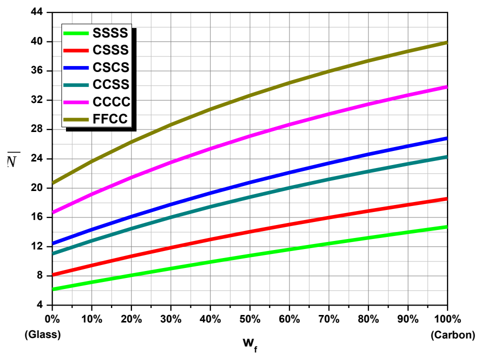

Fig. 4 The boundary conditions effect on the critical buckling load $\bar{N}$ of a square antisymmetric hybrid composite laminates

Table 2 shows a simply supported anti-symmetric cross-ply $(0/90)_n$ square laminated composite plate subjected to mechanical load. Where, a comparison between the results obtained by the various theories and the three-dimensional elasticity solutions given by Noor (1975). It shown from this comparison that the present theory is accurate in precise in predicting the critical buckling loads face to FSDT Whitney (1970), Adim (2016c), Reddy (1984) and exact Noor (1975) theories.

The effect of volume fraction on buckling load of a simply supported antisymmetric Carbon/Glass hybrid laminated composite plate is presented in Table 3 and in Fig. 2. Where the critical buckling load is minimal in the case of full Glass fibers (w_f=100% Glass) and increase gradually according to the fibers percentage w_f until reaching its maximal value for the case of Carbon fibers (w_f =100% Carbon), this is due to the high rigidity of carbon fibers in comparison with Glass ones. Also, the Critical buckling load depend on the volume fraction V_f of the fibers into the total volume of the plate, where, this critical load increase according to the volume fraction augmentation until reaching its peak at V_f =0.45.

In Tables 4-5 and Fig. 3, the side-to-thickness ratio and stacking effects on critical buckling load are presented for a Carbon/Glass hybrid square laminated composite plates. For all cases of combinations between Carbon and Glass fibers, this load increases with the augmentation of stacking (number of layers) and the side to thickness ratio a/h, which is logic because the ratio a/h indicates that there is a condensation of fibers in a small thickness. It is noted that for economic and resistance considerations, the best stacking is eight layers $(0/90)_4$.

Table 6 and Fig. 4 shows the influence of the boundary conditions on the critical buckling loads, where, this load is maximal for the case of free-clamped (FFCC) edges, and minimal for the case of simply supported plates. This shows that the boundary conditions have a major impact on the critical buckling loads of the hybrid composite plates.

The Table 7 represents the variation of the critical buckling load under the aspect ratio a/b and side to thickness ratio a/h effects. For all boundary condition cases, the critical buckling load changes considerably according to the aspect and side to thickness ratios, furthermore, this mean that the plate geometry is a primordial parameter that we should take in consideration in the modeling hybrid composite plates.

8. Conclusions

The Buckling behavior of a Carbon /Glass hybrid laminated composite plate was successfully investigated using a simple and accurate refined shear deformation theory. The accuracy and efficiency of the present theory has been well demonstrated for buckling behavior of antisymmetric cross-ply hybrid composite laminates under different boundary conditions.

The main objective of using the glass and carbon fibers in this study is that, the carbon fibers guaranty a very good mechanical strength, this strength comes with a major impediment which is the expansive cost of this kind of fibers, however glass fibers are less expensive with a low mechanical strength, this is why glass fibers are widely used in most industries (more than 95%). This assembly between these two materials allows to associate in a smart way between the most interesting and required advantages; in one hand, we have the strength provided by the carbon fibers, and in the other hand thanks to the glass fibers we spend less money, where adding a small amount of glass fibers to a carbon fibers based plate allow to reduce significantly the manufacturing cost with only sacrificing a little in terms of strength.

It is up to designers and industrials to choose the proper percentages and amounts in this combination between these two types of fibers to get the maximum benefit of this new technology.

Acknowledgments

This research was supported by the French Ministry of Foreign Affairs and International Development (MAEDI) and Ministry of National Education, Higher Education and Research (MENESR) and by the Algerian Ministry of Higher Education and Scientific Research under Grant No. PHC Tassili 17MDU992. Their support is greatly appreciated. Acknowledgments This research was supported by the French Ministry of Foreign Affairs and International Development (MAEDI) and Ministry of National Education, Higher Education and Research (MENESR) and by the Algerian Ministry of Higher Education and Scientific Research under Grant No. PHC Tassili 17MDU992. Their support is greatly appreciated.

References

Abdelhak, Z., Hadji, L., Hassaine Daouadji, T. and Adda Bedia, E.A. (2015), "Thermal buckling of functionally graded plates using a n-order four variable refined theory", *Adv. Mater. Res.*, **4**(1), 31-44.

Abdelhak, Z., Hadji, L., Hassaine Daouadji, T. and Adda Bedia, E.A. (2016), "Analysis of buckling response of functionally graded sandwich plates using a refined shear deformation theory", *Wind Struct.*, **22**(3), 291-305.

Abualnour, M., Houari, M.S.A., Tounsi, A., Adda Bedia, E.A. and Mahmoud, S.R. (2018), "A novel quasi-3D trigonometric plate theory for free vibration analysis of advanced composite plates", *Compos. Struct.*, **184**, 688-697.

Adim, B., Daouadji, H.T. and Abbes, B. (2016b), "Buckling analysis of antisymmetric cross-ply laminated composite plates under different boundary conditions", *Int. Appl. Mech.*, **52**(6), 126-141.

Adim, B., Daouadji, H.T., Abbes, B. and Rabahi, A. (2016a), "Buckling and free vibration analysis of laminated composite plates using an efficient and simple higher order shear deformation theory", *J. Mech. Industr.*, **17**(5), 512.

Adim, B., Daouadji, H.T. and Rabahi, A. (2016c), "A simple higher order shear deformation theory for mechanical behavior of laminated composite plates", *Int. J. Adv. Struct. Eng.*, **8**(2), 103-117.

Ahouel, M., Houari, M.S.A., Adda Bedia, E.A. and Tounsi, A. (2016), "Size-dependent mechanical behavior of functionally graded trigonometric shear deformable nanobeams including neutral surface position concept", *Steel Compos. Struct.*, **20**(5), 963-981.

Ait Amar Meziane, M., Abdelaziz, H.H. and Tounsi, A. (2014), "An efficient and simple refined theory for buckling and free vibration of exponentially graded sandwich plates under various boundary conditions", *J. Sandw. Struct. Mater.*, **16**(3), 293-318.

Ait Yahia, S., Ait Atmane, H., Houari, M.S.A. and Tounsi, A. (2015), "Wave propagation in functionally graded plates with porosities using various higher-order shear deformation plate theories", *Struct. Eng. Mech.*, **53**(6), 1143-1165.

Al-Basyouni, K.S., Tounsi, A. and Mahmoud, S.R. (2015), "Size dependent bending and vibration analysis of functionally graded micro beams based on modified couple stress theory and neutral surface position", *Compos. Struct.*, **125**, 621-630.

Attia, A., Bousahla, A.A., Tounsi, A., Mahmoud, S.R. and Alwabli Afaf, S. (2018), "A refined four variable plate theory for thermoelastic analysis of FGM plates resting on variable elastic foundations", *Struct. Eng. Mech.*, **65**(4), 453-464.

Belabed, Z., Houari, M.S.A., Tounsi, A., Mahmoud, S.R. and Anwar Bég, O. (2014), "An efficient and simple higher order shear and normal deformation theory for functionally graded material (FGM) plates", *Compos.: Part B*, **60**, 274-283.

Beldjelili, Y., Tounsi, A. and Mahmoud, S.R. (2016), "Hygro-thermo-mechanical bending of S-FGM plates resting on variable elastic foundations using a four-variable trigonometric plate theory", *Smart Struct. Syst.*, **18**(4), 755-786.

Belkorissat, I., Houari, M.S.A., Tounsi, A., Adda Bedia, E.A. and Mahmoud, S.R. (2015), "On vibration properties of functionally graded nano-plate using a new nonlocal refined four variable model", *Steel Compos. Struct.*, **18**(4), 1063-1081.

Bellifa, H., Bakora, A., Tounsi, A., Bousahla, A.A. and Mahmoud, S.R. (2017a), "An efficient and simple four variable refined plate theory for buckling analysis of functionally graded plates", *Steel Compos. Struct.*, **25**(3), 257-270.

Bellifa, H., Benrahou, K.H., Bousahla, A.A., Tounsi, A. and Mahmoud, S.R. (2017b), "A nonlocal zeroth-order shear deformation theory for nonlinear postbuckling of nanobeams", *Struct. Eng. Mech.*, **62**(6), 695-702.

Bellifa, H., Benrahou, K.H., Hadji, L., Houari, M.S.A. and Tounsi, A. (2016), "Bending and free vibration analysis of functionally graded plates using a simple shear deformation theory and the concept the neutral surface position", *J. Braz. Soc. Mech. Sci. Eng.*, **38**(1), 265-275.

Benchohra, M., Driz, H., Bakora, A., Tounsi, A., Adda Bedia, E.A. and Mahmoud, S.R. (2018), "A new quasi-3D sinusoidal shear deformation theory for functionally graded plates", *Struct. Eng. Mech.*, **65**(1), 19-31.

Bennoun, M., Houari, M.S.A. and Tounsi, A. (2016), "A novel five variable refined plate theory for vibration analysis of functionally graded sandwich plates", *Mech. Adv. Mater. Struct.*, **23**(4), 423-431.

Bert, C.W. (1974), *Structure Design and Dnalysis: Part I*, C. C. Chamis (Ed.), Analysis of Plates, Academic Press, New York, U.S.A.

Berthelot, J.M. (2012), *Matériaux Composites: Comportement Mécanique et Analyse des Structures*, Lavoisier, Paris, France.

Besseghier, A., Houari, M.S.A., Tounsi, A. and Mahmoud, S.R. (2017), "Free vibration analysis of embedded nanosize FG plates using a new nonlocal trigonometric shear deformation theory", *Smart Struct. Syst.*, **19**(6), 601-614.

Bhimaraddi, A. and Stevens, L.K. (1984), "A higher order theory for free vibration of orthotropic, homogeneous and laminated rectangular plates", *J. Appl. Mech. Trans. ASME*, **51**(1), 195-198.

Bouderba, B., Houari, M.S.A. and Tounsi, A. (2013), "Thermomechanical bending response of FGM thick plates resting on Winkler-Pasternak elastic foundations", *Steel Compos. Struct.*, **14**(1), 85-104.

Bouderba, B., Houari, M.S.A., Tounsi, A. and Mahmoud, S.R. (2016), "Thermal stability of functionally graded sandwich plates using a simple shear deformation theory", *Struct. Eng. Mech.*, **58**(3), 397-422.

Boukhari, A., Ait Atmane, H., Tounsi, A., Adda Bedia, E.A. and Mahmoud, S.R. (2016), "An efficient shear deformation theory for wave propagation of functionally graded material plates", *Struct. Eng. Mech.*, **57**(5), 837-859.

Bounouara, F., Benrahou, K.H., Belkorissat, I. and Tounsi, A. (2016), "A nonlocal zeroth-order shear deformation theory for free vibration of functionally graded nanoscale plates resting on elastic foundation", *Steel Compos. Struct.*, **20**(2), 227-249.

Bourada, M., Kaci, A., Houari, M.S.A. and Tounsi, A. (2015), "A new simple shear and normal deformations theory for functionally graded beams", *Steel Compos. Struct.*, **18**(2), 409-423.

Bousahla, A.A., Benyoucef, S., Tounsi, A. and Mahmoud, S.R. (2016), "On thermal stability of plates with functionally graded coefficient of thermal expansion", *Struct. Eng. Mech.*, **60**(2), 313-335.

Bousahla, A.A., Houari, M.S.A., Tounsi, A. and Adda Bedia, E.A. (2014), "A novel higher order shear and normal deformation theory based on neutral surface position for bending analysis of advanced composite plates", *Int. J. Comput. Meth.*, **11**(6), 1350082.

Chikh, A., Tounsi, A., Hebali, H. and Mahmoud, S.R. (2017), "Thermal buckling analysis of cross-ply laminated plates using a simplified HSDT", *Smart Struct. Syst.*, **19**(3), 289-297.

Daouadji, H.T. and Adim, B. (2017), "Mechanical behaviour of FGM sandwich plates using a quasi-3D higher order shear and normal deformation theory", *Struct. Eng. Mech.*, **61**(1), 49-63.

Draiche, K., Tounsi, A. and Mahmoud, S.R. (2016), "A refined theory with stretching effect for the flexure analysis of laminated composite plates", *Geomech. Eng.*, **11**(5), 671-690.

El-Haina, F., Bakora, A., Bousahla, A.A., Tounsi, A. and Mahmoud, S.R. (2017), "A simple analytical approach for thermal buckling of thick functionally graded sandwich plates", *Struct. Eng. Mech.*, **63**(5), 585-595.

Hadj Henni, A., Ait Amar, M.M., Bousahla, A.A., Tounsi, A., Mahmoud, S.R. and Alwabli, A.S. (2017), "An efficient hyperbolic shear deformation theory for bending, buckling and free vibration of FGM sandwich plates with various boundary conditions", *Steel Compos. Struct.*, **25**(6), 693-704.

Hamidi, A., Houari, M.S.A., Mahmoud, S.R. and Tounsi, A. (2015), "A sinusoidal plate theory with 5-unknowns and stretching effect for thermomechanical bending of functionally graded sandwich plates", *Steel Compos. Struct.*, **18**(1), 235-253.

Hassaine Daouadji, T. and Hadji, L. (2015), "Analytical solution of nonlinear cylindrical bending for functionally graded plates", *Geomech. Eng.*, **9**(5), 631-644.

Hebali, H., Tounsi, A., Houari, M.S.A., Bessaim, A. and Adda Bedia, E.A. (2014), "New quasi-3D hyperbolic shear deformation theory for the static and free vibration analysis of functionally graded plates", *J. Eng. Mech.*, **140**(2), 374-383.

Jian, W.S., Akihiro, N. and Hiroshi, K. (2004), "Vibration analysis of fully clamped arbitrarily laminated plate", *Compos. Struct.*, **63**(1), 115-122.

Kant, T. and Pandya, B.N. (1988), "A simple finite element formulation of a higher-order theory for unsymmetrically laminated composite plates", *Compos. Struct.*, **9**(3), 215-264.

Khetir, H., Bachir Bouiadjra, M., Houari, M.S.A., Tounsi, A. and Mahmoud, S.R. (2017), "A new nonlocal trigonometric shear deformation theory for thermal buckling analysis of embedded nanosize FG plates", *Struct. Eng. Mech.*, **64**(4), 391-402.

Larbi Chaht, F., Kaci, A., Houari, M.S.A., Tounsi, A., Anwar Bég, O. and Mahmoud, S.R. (2015), "Bending and buckling analyses

of functionally graded material (FGM) size-dependent nanoscale beams including the thickness stretching effect", *Steel Compos*. *Struct*., **18**(2), 425-442.
Levinson, M. (1980), "An accurate, simple theory of the statics and dynamics of elastic plates", *Mech*. *Res*. *Commun*., **7**(6), 343-350.
Librescu, L. (1967), "On the theory of anisotropic elastic shells and plates", *Int*. *J*. *Sol*. *Struct*., **3**(1), 53-68.
Mahi, A., Adda Bedia, E.A. and Tounsi, A. (2015), "A new hyperbolic shear deformation theory for bending and free vibration analysis of isotropic, functionally graded, sandwich and laminated composite plates", *Appl*. *Math*. *Modell*., **39**(9), 2489-2508.
Menasria, A., Bouhadra, A., Tounsi, A., Bousahla, A.A. and Mahmoud S.R. (2017), "A new and simple HSDT for thermal stability analysis of FG sandwich plates", *Steel Compos*. *Struct*., **25**(2), 157-175.
Mindlin, R.D. (1951), "Influence of rotary inertia and shear on flexural motions of isotropic, elastic plates", *J*. *Appl*. *Mech*. *Trans*. *ASME*, **18**(1), 31-38.
Nedri, K., El Meiche, N. and Tounsi, A. (2014), "Free vibration analysis of laminated composite plates resting on elastic foundation by using a refined hyperbolic shear deformation theory", *Mech*. *Compos*. *Mater*., **49**(6), 629-640.
Noor, A.K. (1975), "Stability of multilayered composite plate", *Fibre Sci*. *Technol*., **8**(2), 81-89.
Ould Youcef, D., Kaci, A., Benzair, A., Bousahla, A.A. and Tounsi, A. (2018), "Dynamic analysis of nanoscale beams including surface stress effects", *Smart Struct*. *Syst*., **21**(1), 65-74.
Reddy, J.N. (1986), "A simple higher-order theory for laminated composite plates", *J*. *Appl*. *Mech*. *Trans*. *ASME*, **51**(4), 745-752.
Reissner, E. (1945), "The effect of transverse shear deformation on the bending of elastic plates", *J*. *Appl*. *Mech*. *Trans*. *ASME*, **12**(2), 69-77.
Ren, J.G. (1986), "A new theory of laminated plate", *Compos*. *Sci*. *Technol*., **26**(3), 225-239.
Srinivas, S. and Rao, A.K. (1970), "Bending, vibration and buckling of simply supported thick orthotropic rectangular plates and laminates", *Int*. *J*. *Sol*. *Struct*., **6**(11), 1463-1481.
Thai, H.T. and Choi, D.H. (2013), "A simple first-order shear deformation theory for laminated composite plates", *Compos*. *Struct*., **106**, 754-763.
Tlidji, Y., Hassaine Daouadji, T., Hadji, L. and Adda Bedia, E.A. (2014), "Elasticity solution for bending response of functionally graded sandwich plates under thermo mechanical loading", *J*. *Therm*. *Stress*, **37**(7), 852-869.
Tounsi, A., Houari, M.S.A., Benyoucef, S. and Adda Bedia, E.A. (2013), "A refined trigonometric shear deformation theory for thermoelastic bending of functionally graded sandwich plates", *Aerospace Sci*. *Technol*., **24**(1), 209-220.
Vasiliev, V.V. and Morozov, E.V. (2001), *Mechanics and Analysis of Composite Materials*. Oxford, Elsevier Science.
Whitney, J.M. and Sun, C.T. (1973), "A higher-order theory for extensional motion of laminated composites", *J*. *Sound Vibr*., **30**(1), 85-97.
Whitney, J.M. and Pagano, N.J. (1970), "Shear deformation in heterogeneous anisotropic plates", *J*. *Appl*. *Mech*. *Trans*. *ASME*, **37**(4), 1031-1036.
Yazid, M., Heireche, H., Tounsi, A., Bousahla, A.A. and Sid Ahmed, M.H. (2018), "A novel nonlocal refined plate theory for stability response of orthotropic single-layer graphene sheet resting on elastic medium", *Smart Struct*. *Syst*., **21**(1), 15-25.
Zemri, A., Houari, M.S.A., Bousahla, A.A. and Tounsi, A. (2015), "A mechanical response of functionally graded nanoscale beam: an assessment of a refined nonlocal shear deformation theory beam theory", *Struct*. *Eng*. *Mech*., **54**(4), 693-710.
Zidi, M., Tounsi, A., Houari, M.S.A., Adda Bedia, E.A. and Anwar Bég, O. (2014), "Bending analysis of FGM plates under hygro-thermo-mechanical loading using a four variable refined plate theory", *Aerospace Sci*. *Technol*., **34**, 24-34.
Zine, A, Tounsi, A., Draiche, K., Sekkal, M. and Mahmoud, S.R. (2018), "A novel higher-order shear deformation theory for bending and free vibration analysis of isotropic and multilayered plates and shells", *Steel Compos*. *Struct*., **26**(2), 125-137.

CC